# Eddy Current Loss Effect in Foil Winding of Transformer Based on Magneto-Fluid-Thermal Simulation

Yongjian Li[1,2], Xinxiao Yan[1,2], Chunguang Wang[3], Qingxin Yang[1,2,4], and Changgeng Zhang[1,2]

[1]State Key Laboratory of EERI, School of Electrical Engineering, Hebei University of Technology, Tianjin 300130, China
[2]Hebei Province Key Laboratory of EFEAR, Hebei University of Technology, Tianjin 300130, China
[3]TBEA Tianjin Transformers Company Ltd., Tianjin 300450, China
[4]School of Electrical Engineering, Tianjin University of Technology, Tianjin 300384, China

**The foil winding temperature distribution is crucial to the life of power transformer since local heating can accelerate aging of insulation materials. However, based on the traditional 3-D electromagnetic model and the principle of heat transfer, the non-uniform losses and temperature distribution of foil windings are difficult to estimate because of complex magnetic leakage flux. In this paper, the magneto-fluid-thermal coupling model has been established to calculate the temperature rise and predict the potential hotspots of a simplified dry-type power transformer rated at 2500 kVA. Moreover, the influence of insulation barrier is considered to reshape the air-flow path and to affect the radiative effect between the high-voltage and low-voltage windings. Experimental temperature rises are measured with infrared thermography to verify the simulation results, which achieved reasonable hotspot predictions and provide the theoretical method for transformer designers.**

*Index Terms*—**Dry-type transformer, magneto-fluid-thermal coupling, stray loss, temperature rise.**

## I. Introduction

As A critical equipment for energy transmission, the reliability of power transformers is crucial to power systems. Thermal effect is one of the main reasons causing transformer failures since local heating can destroy the insulation structure [1], [2]. Nowadays, calculation for the additional losses in the windings of large-capacity power transformer should not be ignored. In particular, the extremely non-uniformity of the power losses in foil windings due to induced current can drastically shorten transformer lifespan. Conventional analytical model such as Dowell [3] and Biro [4] is widely used for loss calculation and thermal design, in which simplified geometries are solved to characterize the skin and proximity effects. With the advanced development of 3-D finite-element method (FEM), the **A-V-A** and **T-Ω** methods have been applied in the eddy current field problems such as non-linearity and non-uniform conductivity in the conductor region [5]. Thermohydraulic or thermal network models are usually considered for temperature calculation and thermal design. A key problem in the thermal analysis of dry-type transformer is the complexity of geometrical shape such as the insulation layer, air duct which needs to be homogenous processed avoiding the ultra-dense mesh. In addition, the heat transfer coefficients in the surface of winding air duct are dependent on the temperature distribution of air, which is difficult to be accurately evaluated with empirical formulas [6]. The algorithm for multi-physics field is applied to calculate the convective heat transfer coefficient of the fluid–solid coupling interface.

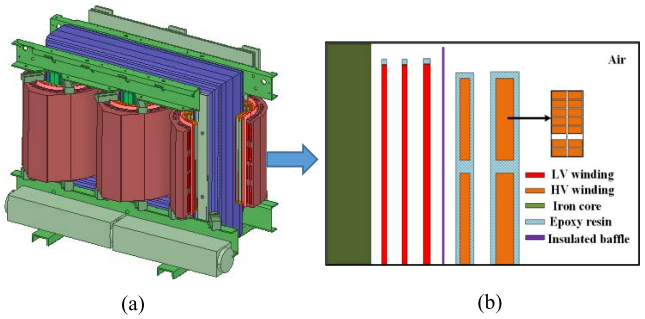



Fig. 1. Dry-type model of power transformer. (a) Geometry model of the three-phase transformer. (b) Cross-sectional view of winding.

In this paper, a 3-D magneto-fluid-thermal transient simulation model is established to research the non-uniform losses distribution of foil windings, stranded windings, and transformer core caused by leakage flux. The simulation results including temperature rise and hotspots of a dry-type transformer under natural convection cooling are verified by short-circuit experiments with the infrared thermography.

## II. Transformer Model and Finite-Element Simulation

### A. Magneto-Fluid-Thermal Coupling Model

A dry-type transformer model with a rated capacity of 2500 kVA is built up as shown in Fig. 1(a), the cross-sectional view can be observed in Fig. 1(b). Foil windings are applied for the low-voltage (LV) side, while disk-shaped copper wires are used for the high voltage (HV). Each HV winding is divided into four sections in the axial direction to enlarge the area to dissipate heat by convection and radiation. The insulated end rings are placed at the end of the primary windings. In addition, the insulation barrier used for electrical

Manuscript received November 5, 2018; revised January 25, 2019; accepted January 28, 2019. Date of publication March 4, 2019; date of current version June 20, 2019. Corresponding author: C. Zhang (e-mail: changgenng.zhang@hebut.edu.cn).

Color versions of one or more of the figures in this paper are available online at http://ieeexplore.ieee.org.

Digital Object Identifier 10.1109/TMAG.2019.2897503

0018-9464 © 2019 IEEE. Personal use is permitted, but republication/redistribution requires IEEE permission.
See http://www.ieee.org/publications_standards/publications/rights/index.html for more information.

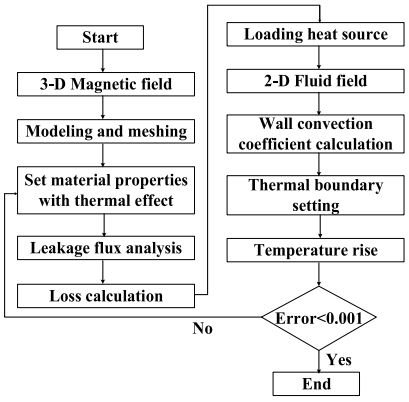



Fig. 2. Flowchart of magneto-fluid-thermal coupling model.

isolation is placed between HV and LV sides, which would also affect the convective and radiant heat dissipation.

### B. Numerical Analysis of Eddy Current

Based on the simplified transformer structure, a multi-physic model is built up to calculate the non-uniform power losses and temperature rise distribution as shown in Fig. 2. The total loss of power transformer windings comprises ohmic loss of HV and LV windings, stray loss, eddy current loss of windings, and core loss. For ultra-thin foil windings, the radial leakage flux makes it non-uniform eddy current distribution. These various kinds of power losses are solved by non-linear and magnetic anisotropy Maxwell's equations as following [5]:

$$\nabla \times (\boldsymbol{v}\nabla \times \boldsymbol{A}) = -\boldsymbol{J}_s + \boldsymbol{J}_e \tag{1}$$

$$\boldsymbol{J}_e = -\sigma_e \frac{\partial \boldsymbol{A}}{\partial t} + \nabla \boldsymbol{V} \tag{2}$$

where $\boldsymbol{A}$ is the magnetic vector potential, $V$is the electric scalar potential, $v$ is the magnetic reluctivity tensor, $\boldsymbol{J}_s$ is the source current density of the conductor, $\boldsymbol{J}_e$ is the eddy current density induced by leakage flux, and $\sigma_e$ is the electric conductivity. The mechanical components such as pull plates and other small bolts can be neglected in the electromagnetic simulation due to the small impact on heat source and temperature distribution.

The HV windings are wound by rectangle-shaped copper wires. Under full-load operation, the internal cross section of the single wire will produce additional loss associated with the skin and proximity effects; however, it is too much computational burden for FEM to refine mesh in each stranded coil. The stranded coils are modeled into a homogenous copper block, in which the eddy current loss is analytically computed considering the shape of each stranded coil expressed as [7]

$$P_w = \frac{\pi D_{av} mnba^3 \omega^2 B_p^2}{72\rho_T} \tag{3}$$

where $B_p$ is the peak value of magnetic flux density, $D_{\text{av}}$ is the average diameter of disk-shaped copper coil, $\rho_T$ is the resistivity at the temperature of $T$, and the other parameters are denoted in Fig. 3. The eddy current in the stranded HV coils can be estimated by the simplified post-processing (3) with the local leakage flux density much more exactly than by the method of empirical correction coefficient to the dc stranded loss.

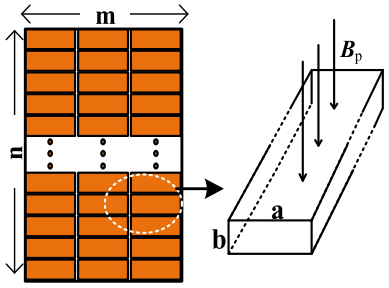



Fig. 3. Schematic of a block of HV coil.

### C. Thermal Numerical Model

*1) Thermal Conduction in Solid Domain:* Based on the principle of heat transfer, the solution of heat conduction differential equation for steady-state temperature field in 2-D Cartesian coordinate system can be simulated as a boundary value problem [2]

$$\begin{cases} \dfrac{\partial}{\partial x}\left(k_x \dfrac{\partial T}{\partial x}\right) + \dfrac{\partial}{\partial y}\left(k_y \dfrac{\partial T}{\partial y}\right) + Q = \rho c_{\text{p}} \dfrac{\partial T}{\partial t} \\ T\,|L_1 = T_0 \end{cases} \tag{4}$$

where $k_x$ and $k_y$ represent thermal conductivity of the solid object in the $x$-and $y$-directions, $Q$ is the heat source term, $\rho$ is the mass density, $c_p$ is the specific heat, $\alpha$ is the convective heat dissipation coefficient, $L_1$ is the fluid–solid coupling boundary, and $T_0$ is the boundary temperature.

The LV coil is made of copper foil and insulated prepreg paper, while the HV coil is composed of copper wires, insulation coating, glass fiber, and so on. Thermal conductivity for multi-media heat-conducting region differs greatly. For foil windings, the radial equivalent thermal conductivity can be obtained as follows [8]:

$$\lambda_r = \frac{\lambda_1 \lambda_2 (d_1 + d_2)}{d_1 \lambda_1 + d_2 \lambda_2}. \tag{5}$$

The axial equivalent thermal conductivity is

$$\lambda_a = \frac{(\lambda_1 d_1 + \lambda_2 d_2)}{d_1 + d_2} \tag{6}$$

where $\lambda_1$ and $\lambda_2$ represent thermal conductivity of copper and insulation materials and $d_1$ and $d_2$ are the thickness of them.

*2) Thermal Convection and Radiation in Fluid Domain:* Considering the changing of air density due to temperature rise of dry-type transformer, Boussinesq hypothesis is set up. It assumes that fluid density is constant in all other momentum conservation equations except for volumetric force term [8]

$$\rho\left(\frac{\partial \boldsymbol{u}}{\partial t} + \boldsymbol{u}\nabla \cdot \boldsymbol{u}\right) = -\nabla p + \nabla \cdot \boldsymbol{\tau} - \rho \mathbf{g} + \boldsymbol{F} \tag{7}$$

$$(\rho - \rho_0)\boldsymbol{g} = -\rho_0 \beta (T - T_0)\boldsymbol{g} \tag{8}$$

where $\boldsymbol{u}$ is the velocity of air, $\tau$ is the stress tensor, $p$ is the static pressure, $\rho$ is the air density, and $\boldsymbol{F}$ is the applied body force. In the body force terms, the fluid density is linear just as (8), where $\rho_0$is the constant air density and $\beta$ is the body expansion coefficient.

The surfaces of HV coil, LV coil, and insulated barrier radiate and absorb heat at the same time. The static heat transfer

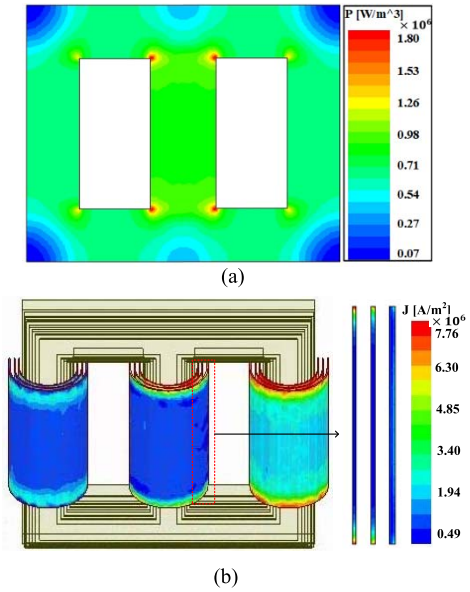



Fig. 4. Simulation loss for transformer core and windings. (a) Simulated total loss density distribution in the core of transformer. (b) Current density distribution for the global model when the C-phase winding is excited to the maximum value.

can be calculated by the Stephen Boltzmann equation [8]

$$q = \frac{\sigma_b (T_1^4 - T_2^4)}{(1/\varepsilon_1) + ((1-\varepsilon_2)/\varepsilon_2)(R_1/R_2)} \tag{9}$$

where $q$ is the heat flow rate, $\varepsilon_1$ and $\varepsilon_2$ are the emissivities of the first and second surface, respectively, $\sigma_b$ is the radiative constant of blackbody, $\sigma_b = 5.67 \times 10^{-8}\mathrm{W/(m^2 \cdot K^4)}$, $R_1$ and $R_2$ are the radius of the inner and outer radiant surfaces, and $T_1$ and $T_2$ represent the absolute temperatures of radiative surfaces.

## III. Numerical Solutions

### A. Electromagnetic Simulation of Power Transformer

To ensure the closure and integrity of the magnetic circuit, the FEM analysis for 3-D transformer model had been carried out under full-load condition. The rated current is set 3.61 kA for LV coils and 83.3 A for HV coils in the simulation based on the short-circuit experiment. Fig. 4(a) shows the calculated core loss density in the cross section of the core at 50 Hz. Classical Steinmetz equation is adopted for core loss calculation [7]

$$P_{\mathrm{Fe}} = k_h f B_m + k_c f B_m + k_e (f B_m)^{1.5} \tag{10}$$

where $k_{\mathrm{h}}$, $k_{\mathrm{c}}$, and $k_e$ represent the coefficients of alternating hysteresis loss, eddy current loss, and excess loss, respectively. It can be seen that the maximum power loss is found at the corner of T-shaped joint, which is result from large magnetic flux density and rotational magnetization.

Fig. 4(b) displays the current density distribution of foil windings when the C-phase is excited by the maximum current. It can be seen that the current density in the middle of the winding is relatively stable but increases dramatically at both edges due to the induced current, especially for the innermost layer. Compared with the calculated design value of $2.13 \times 10^6$ (A/m$^2$), the maximum value can be up to 3.64 times that of applied source current density, the minimum reaches 0.6 times since the further away from the core, the weaker the magnetic flux leakage.

TABLE I
THERMAL PARAMETER DATA OF THE MODEL

| Model | Material | Thermal Conductivity [W/(m· K)] | Specific Heat [J/(kg· K)] | Density [kg/m$^3$] |
|---|---|---|---|---|
| Core | 30QG120 | x = y = 20 | 502.48 | 7650 |
| Low-voltage winding | copper foil | $x$ = 1.99<br>$y$ = 318 | 381 | 8978 |
| High-voltage winding | copper | $x$ = 1.19<br>$y$ = 4.82 | 381 | 8978 |
| Insulation | epoxy resin | x = y = 0.267 | 1970 | 1.16 |
| Isolation barrier | Polyester Composite Film | x = y = 0.035 | --- | 50 |

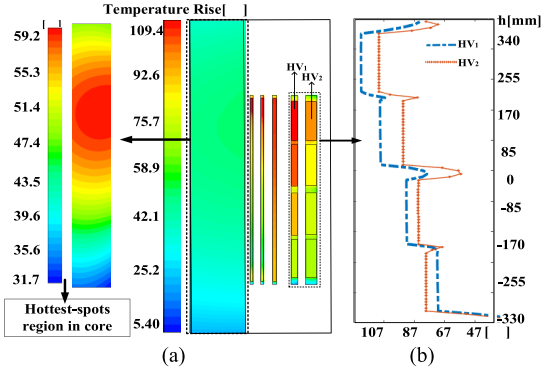



Fig. 5. Transformer temperature distribution without insulation barrier. (a) Temperature distribution. (b) Comparison of temperature rise for different parts.

## IV. Computation Fluid Dynamics Considering Insulation Barrier

The thermal parameters of the model are calculated according to (7) and (8), as shown in Table I. It has been assumed that temperature rise of the winding has no abrupt change along the circumferential direction, so the 2-D axisymmetric model is set up for temperature field calculation. In the computation of the thermal field, the ambient temperature is set to 20 °C and the pressure on outlet boundary is defined as one standard atmospheric pressure; the thermal conductivity of windings is set to be anisotropic.

### A. Simulation Results Without Insulation Barrier

The total loss calculated in FEM is transferred into the computational fluid dynamic (CFD) software element by element, in which the heat transfer coefficient is iteratively calculated. Fig. 5 shows the temperature distribution of the transformer model and axial temperature rise curve of HV windings under natural convection cooling. It can be seen that the amount of heat is concentrated in the upper part of the transformer. The average temperature in the inner surfaces of the first segment HV windings can be up to 107 °C, which is the key part for the thermal design.

Fig. 6 shows the distribution of air-flow velocity without insulation barrier. The heated air flow expands and rises in

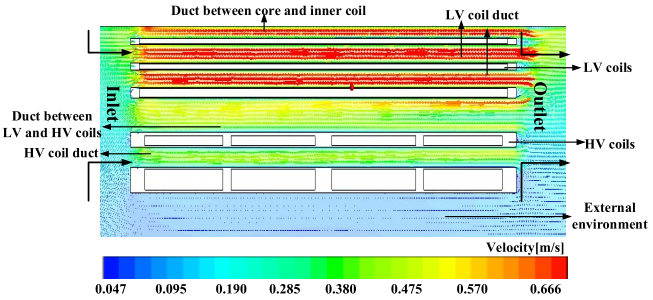



Fig. 6. Distribution of air-flow velocity without insulation barrier.

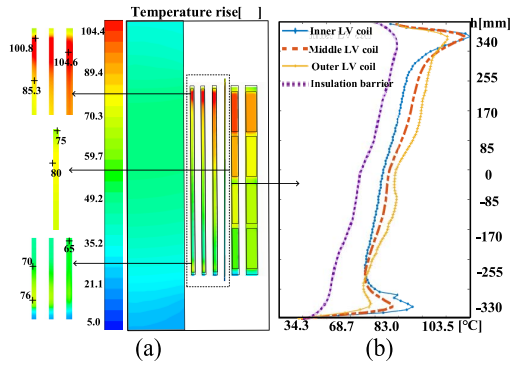



Fig. 7. Transformer temperature distribution with insulation barrier. (a) Temperature distribution (b) Comparison of temperature rise for different parts.

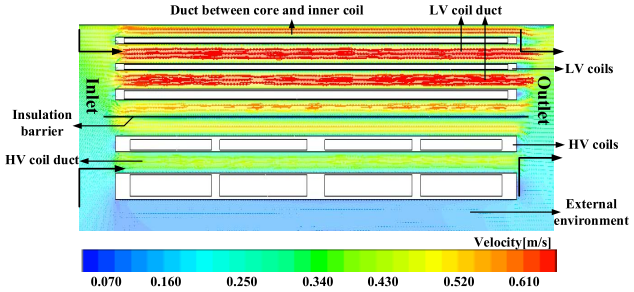



Fig. 8. Velocity of air flow in the LV and HV coil duct with insulation barrier.

the air duct, which maximum velocity can be up to 0.67 m/s. The temperature rise in the upper region is higher than that in the lower region. The radiant energy between the surfaces inside the air duct is much smaller than that in the outermost surface of the HV winding, which radiate heat is dissipated to the external environment.

### *B. Simulation Results With Insulation Barrier*

An insulation barrier with a height of 720 mm and a thickness of 1.1 mm is designed to reshape the air-flow path. Fig. 7 illustrates the temperature rise and axial temperature rise curve in LV windings with the improved design. The peak of the temperature curve appears at the end of foil winding, which is mainly attributed to the eddy current loss induced by leakage flux. Compared with the original results, the average temperature rise of the winding drops by 5 °C. With the absorption of radiant energy, the temperature rise of insulation barrier can be up to 75 °C. Fig. 8 shows the variation in flow velocity distribution due to changes of the air duct structure.

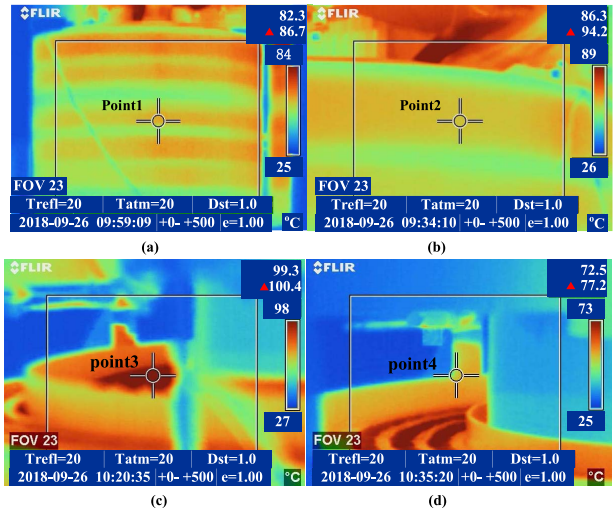



Fig. 9. Experimental temperature distribution by an infrared thermography. (a) Over HV windings. (b) End of outer HV windings. (c) End of foil windings. (d) End of insulation barrier.

TABLE II
TESTED AND SIMULATED OF TEMPERATURE RISE

| Measured points | point1 | point2 | point3 | point4 |
|---|---|---|---|---|
| Tested[°C] | 84 | 89 | 98 | 73 |
| Simulated[°C] | 87.3 | 93 | 100.8 | 75 |

### *C. Experimental Results*

In order to verify the simulation results, the temperature rise experiment under short-circuit condition has been carried out. In the test, the temperatures at the end of foil windings and the outer region of HV windings are measured by using an infrared thermography as shown in Fig. 9. Table II gives the comparison between tested temperature and simulated value of the points shown in Fig. 9(a)–(d). Compared with the simulation results in Figs. 6(b) and 8(b) as well as Table II, it can be proved that the prediction of hotspots by multi-physics coupling simulation is in good agreement with the measurement results. The major errors mainly come from that the 3-D shape of the air duct increases the convective heat dissipation area, which cannot be taken into account in 2-D CFDs. As a result, the magneto-fluid-thermal calculated values are slightly larger than the measured ones.

## V. CONCLUSION

A coupled magneto-fluid-thermal model is established to calculate the temperature rise of power transformer accurately. Combined electromagnetic FEM and analytical equation, the non-uniform loss distribution of core, foil windings, and stranded winding can be obtained. The coupled simulation shows that the temperature rise of the LV coil is higher than that of the HV coil. The hottest spots appear in the upper part of the outer layer of LV windings and inner layer of HV wingdings. When the insulation barrier is taken into account, temperature rise decreases 5 °C. The coupling simulation results are in good agreement with the measured

data, which can prove that the proposed method is efficient for optimization of transformer.

## ACKNOWLEDGMENT

This work was supported in part by the National Natural Science Foundation of China under Grant 51807048, Grant 51777055, and Grant 51690181, in part by Hebei Province Science Foundation under Grant E2018202284 and Grant E2018202301, in part by Scholarship from China Scholarship Council under Grant 201806705006, and in part by the Scientific Research Project of Hebei University under Grant QN2018157.

## REFERENCES

[1] M. Xiao and B. X. Du, "Effects of high thermal conductivity on temperature rise of epoxy cast winding for power transformer," *IEEE Trans. Dielectr. Electr. Insul.*, vol. 23, no. 4, pp. 2413–2420, Aug. 2016.

[2] J. Smolka and A. J. Nowak, "Experimental validation of the coupled fluid flow, heat transfer and electromagnetic numerical model of the medium-power dry-type electrical transformer," *Int. J. Therm. Sci.*, vol. 47, no. 10, pp. 1393–1410, 2008.

[3] P. L. Dowell, "Effects of eddy currents in transformer windings," *Proc. Inst. Elect. Eng.*, vol. 113, no. 8, pp. 1387–1394, Aug. 1966.

[4] O. Biro, K. Preis, W. Renhart, K. R. Richter, and G. Vrisk, "Performance of different vector potential formulations in solving multiply connected 3-D eddy current problems," *IEEE Trans. Magn.*, vol. 26, no. 2, pp. 438–441, Mar. 1990.

[5] M. Lee, H. A. Abdullah, J. C. Jofriet, and D. Patel, "Temperature distribution in foil winding for ventilated dry-type power transformers," *Electr. Power Syst. Res.*, vol. 80, no. 9, pp. 1065–1073, 2010.

[6] M. Lee, H. A. Abdullah, J. C. Jofriet, D. Patel, and M. Fahrioglu, "Air temperature effect on thermal models for ventilated dry-type transformers," *Electric Power Syst. Res.*, vol. 81, no. 3, pp. 783–789, 2011.

[7] C. B. Vaughinski, *Transformer Theory and Calculation*. Beijing, China: Mechanical Industry Press, 1983.

[8] F. P. Incropera, D. P. Dewitt, T. L. Bergman, and A. S. Lavine, *Fundamentals of Heat and Mass Transfer*. Beijing, China: Chemical Industry Press, 2007.